Supporting Information (SI)

Phosphazene Base-Mediated Azide-Alkyne Click Polymerization toward 1,5-Regioregular Polytriazoles

Baixue Li,[†] Yong Liu,[†] Han Nie,[†] Anjun Qin[†] and Ben Zhong Tang*[†‡]*

[†] State Key Laboratory of Luminescent Materials and Devices, Center for Aggregation-Induced Emission, South China University of Technology, Guangzhou 510640, China.

[‡] Department of Chemistry, Hong Kong Branch of Chinese National Engineering Research Center for Tissue Restoration and Reconstruction, Institute for Advanced Study, and Department of Chemical and Biological Engineering, The Hong Kong University of Science & Technology, Clear Water Bay, Kowloon, Hong Kong, China.

Table of Contents

Synthesis procedures of monomers 1a and 1b.

Synthesis of 4,4'-diazidobiphenyl (1a)

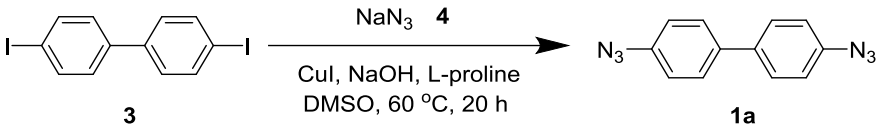

This monomer was prepared according to our previously published procedures.[1]

Synthesis of 1,6-bis(4-azidophenoxy)hexane (1b)

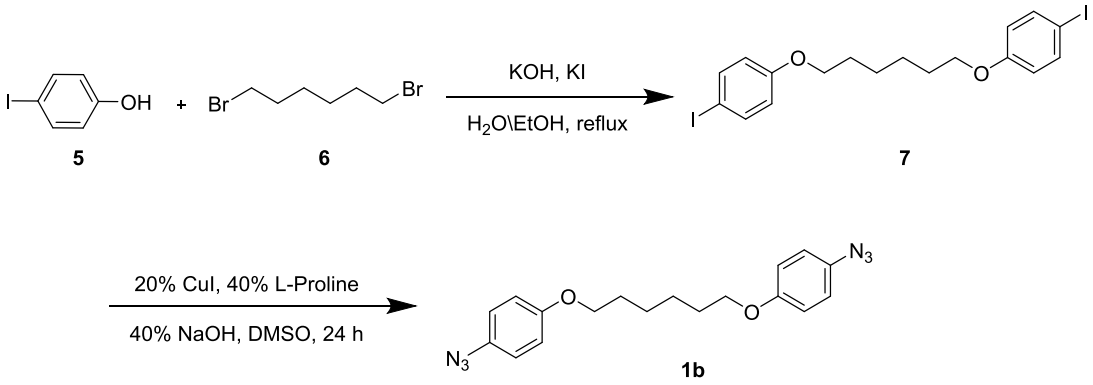

This monomer was prepared according to our previously published procedures.[2]

Synthesis procedures of monomers 2a-2c.

Synthesis of 4,4′-(Isopropylidenediphenyl)-bis(4-ethynylbenzyl) ether (2a)

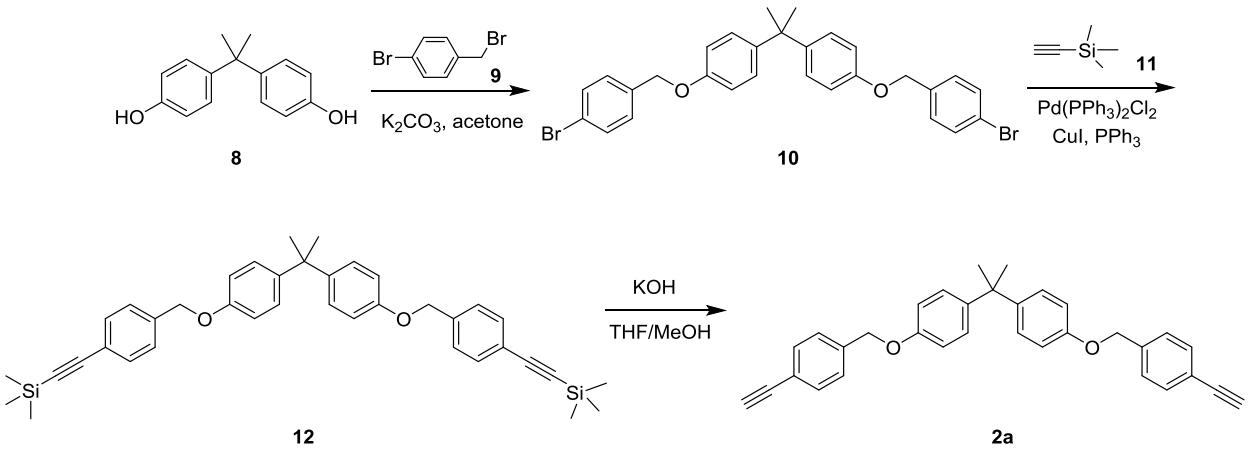

This monomer was prepared according to our previously published procedures.[3,4]

Synthesis of 1,2-bis(4-ethynylphenyl)-1,2-diphenylethene (2b)

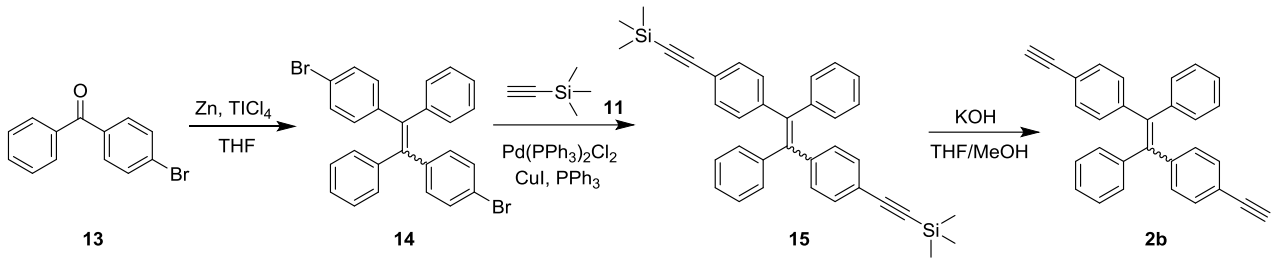

This monomer was prepared according to our previously published procedures.[3,4]

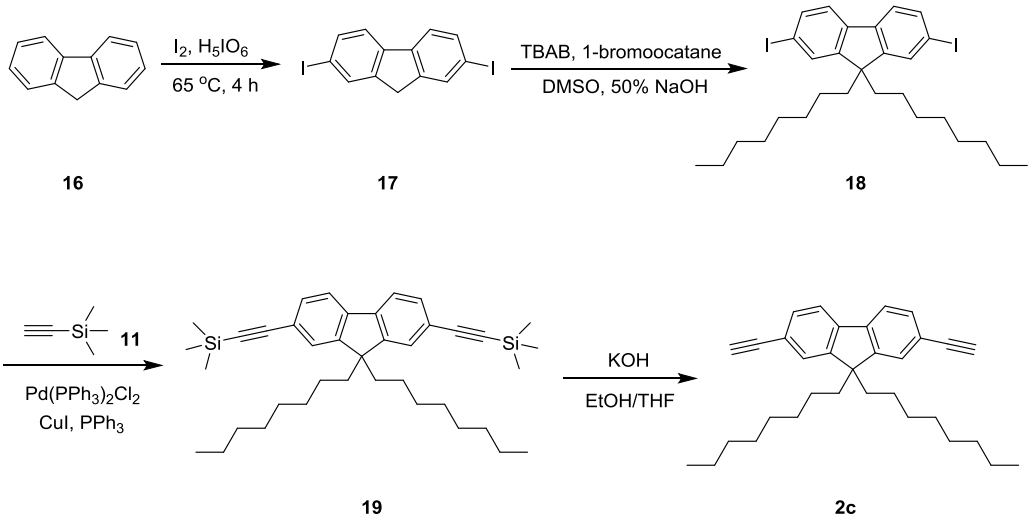

This monomer was prepared according to our previously published procedures.[5]

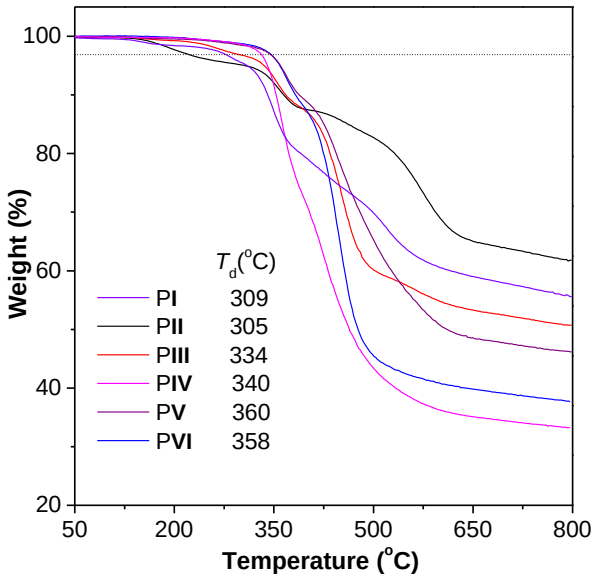

Figure S1. TGA curves of P**I**-P**VI**. T_d presents the temperature of 5% weight loss.

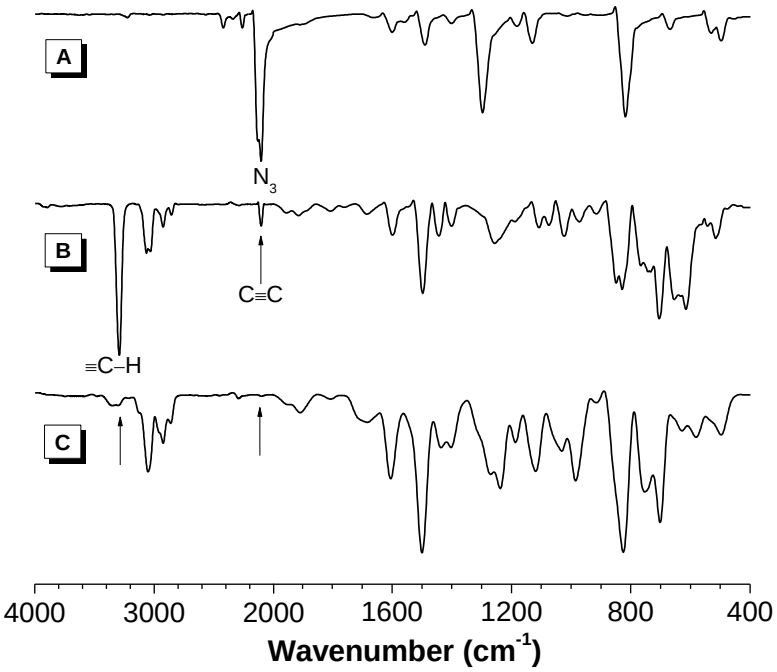

Figure S2. FT-IR spectra of **1a** (A), **2b** (B) and P**II** (C).

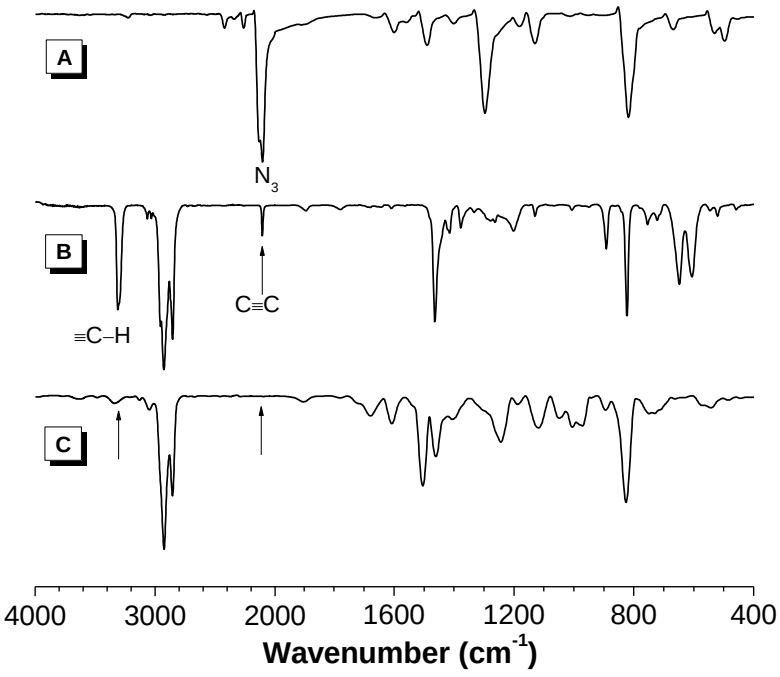

Figure S3. FT-IR spectra of **1a** (A), **2c** (B) and P**III** (C).

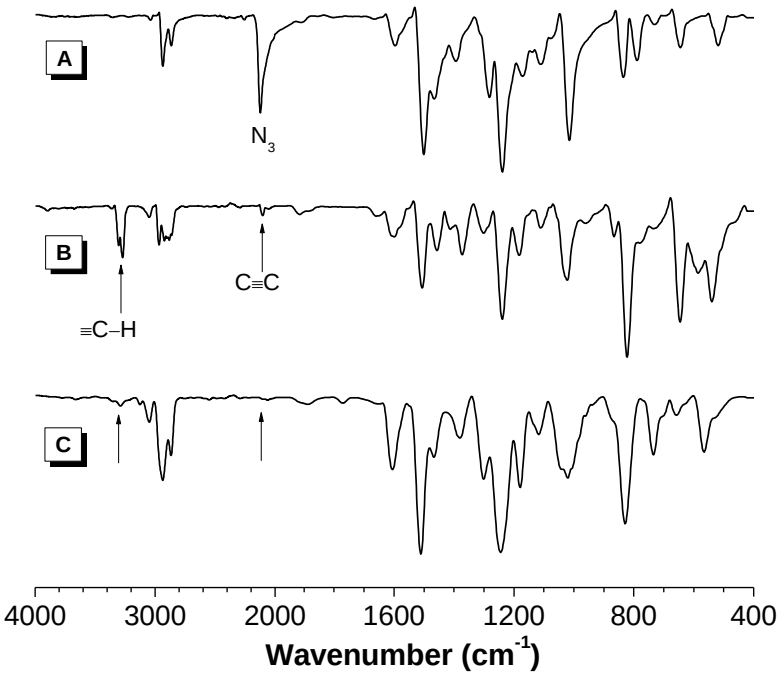

Figure S4. FT-IR spectra of **1b** (A), **2a** (B) and P**IV** (C).

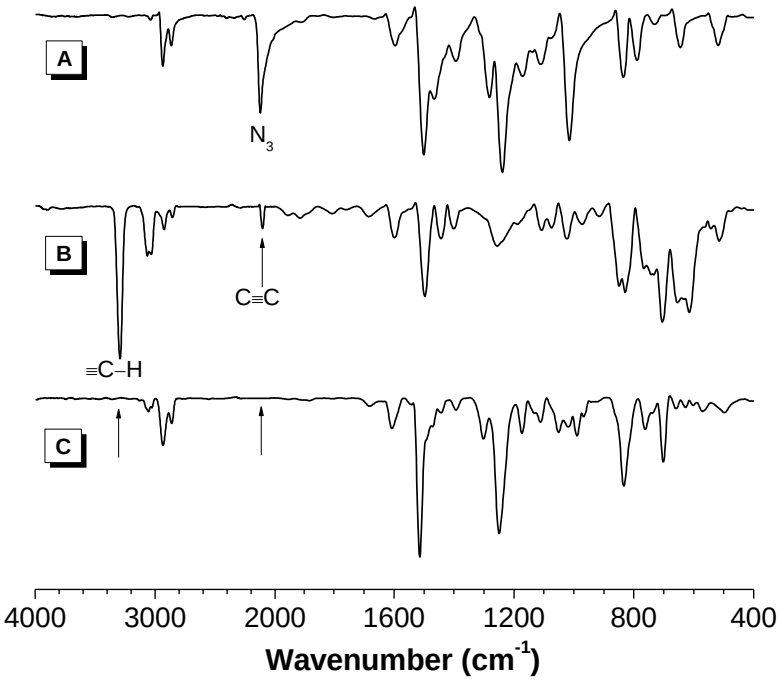

Figure S5. FT-IR spectra of **1b** (A), **2b** (B) and P**V** (C).

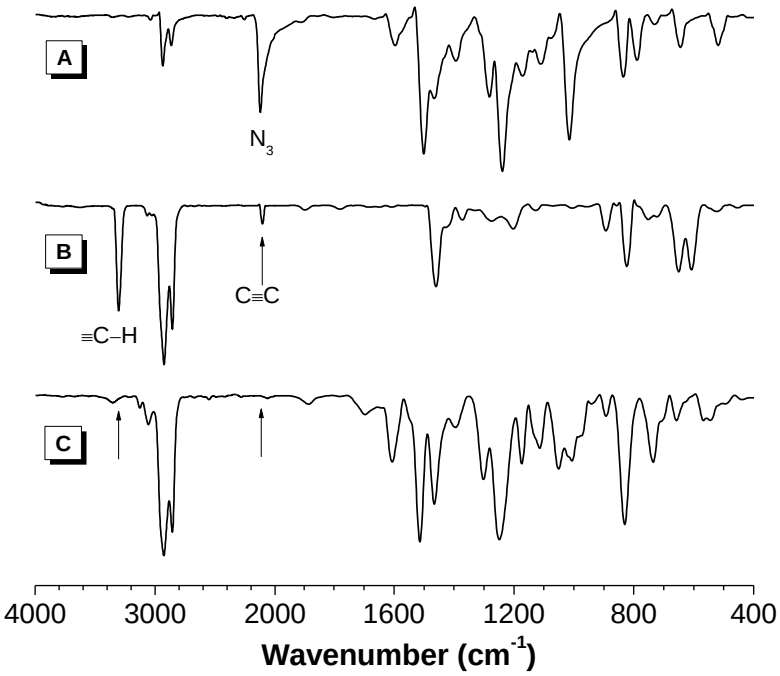

Figure S6. FT-IR spectra of **1b** (A), **2c** (B) and P**VI** (C).

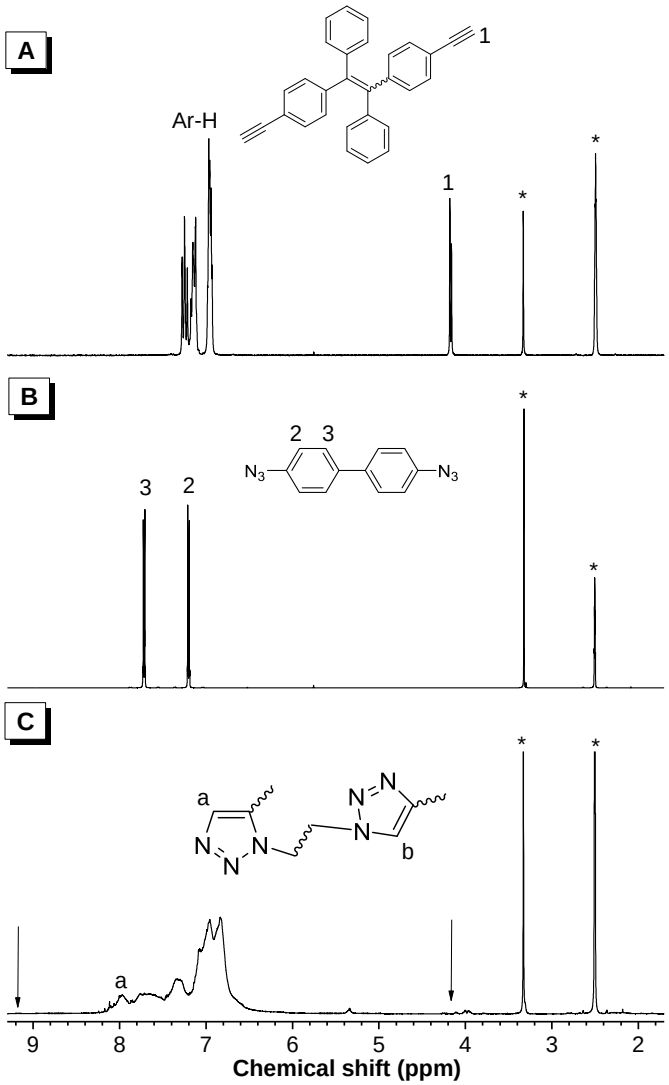

Figure S7. ^{1}H NMR spectra of **2b** (A), **1a** (B) and P**II** (C) in DMSO-d_6. The solvent peaks are marked with asterisks.

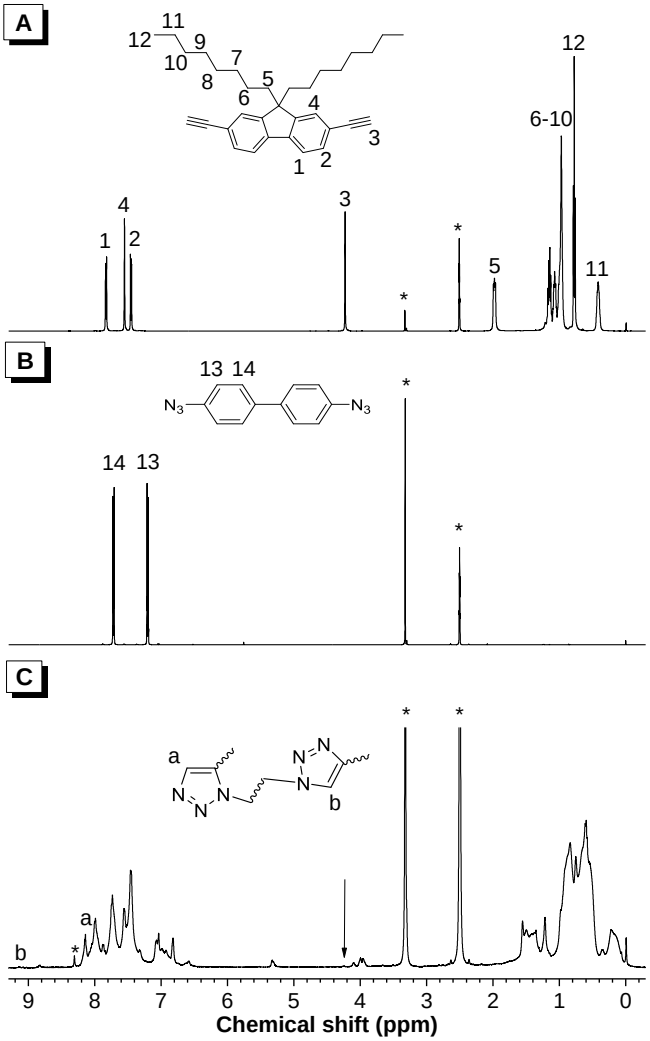

Figure S8. [1]H NMR spectra of **2c** (A), **1a** (B) and P**III** (C) in DMSO-d_6. The solvent peaks are marked with asterisks.

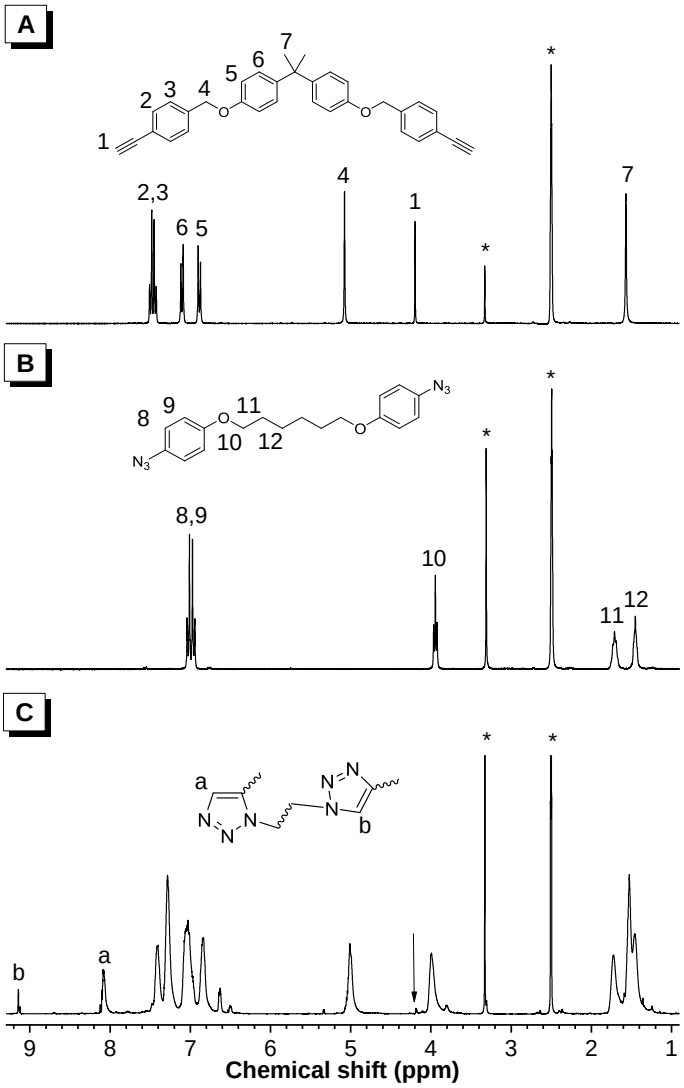

Figure S9. ^{1}H NMR spectra of **2a** (A), **1b** (B) and P**IV** (C) in DMSO-d_6. The solvent peaks are marked with asterisks.

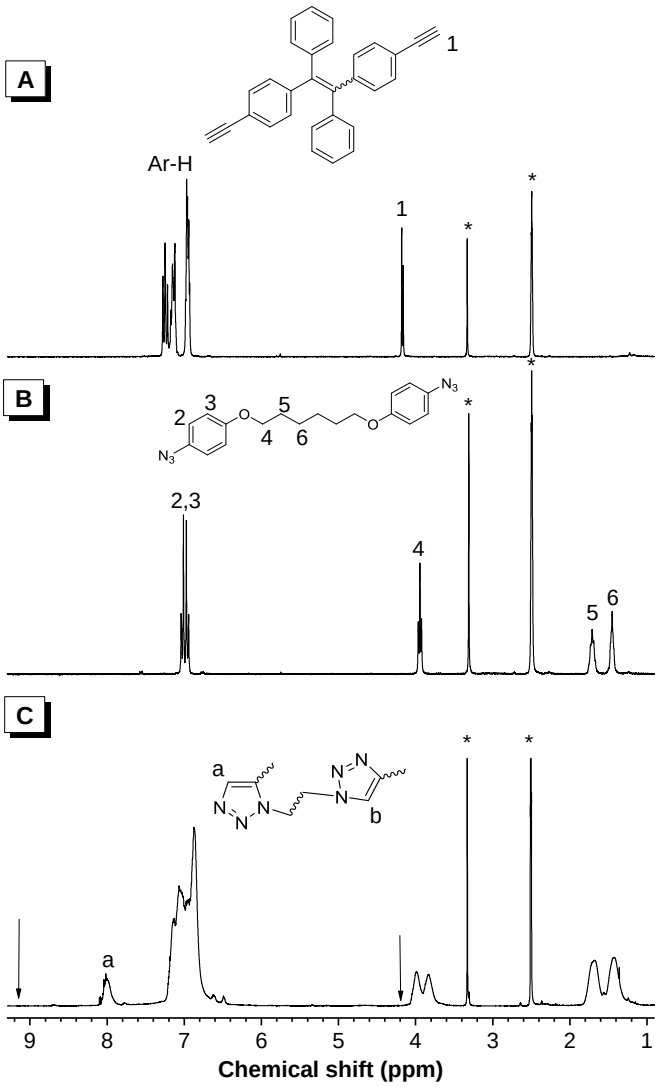

Figure S10. ^{1}H NMR spectra of **2b** (A), **1b** (B) and P**V** (C) in DMSO-d_6. The solvent peaks are marked with asterisks.

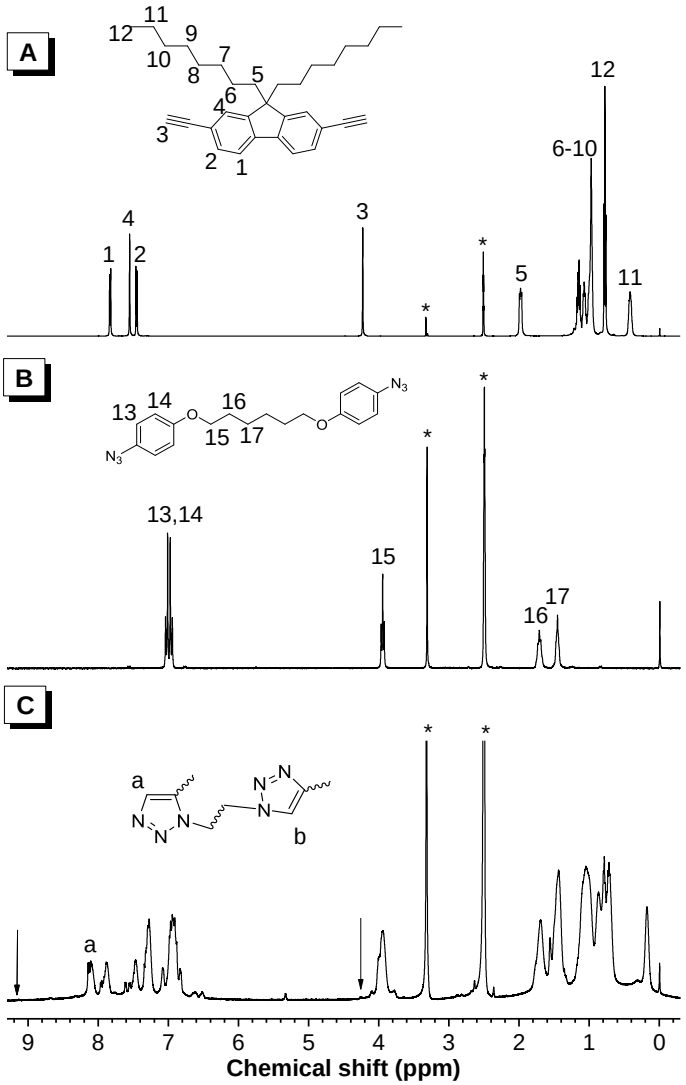

Figure S11. ^{1}H NMR spectra of **2c** (A), **1b** (B) and P**VI** (C) in DMSO-d_6. The solvent peaks are marked with asterisks.

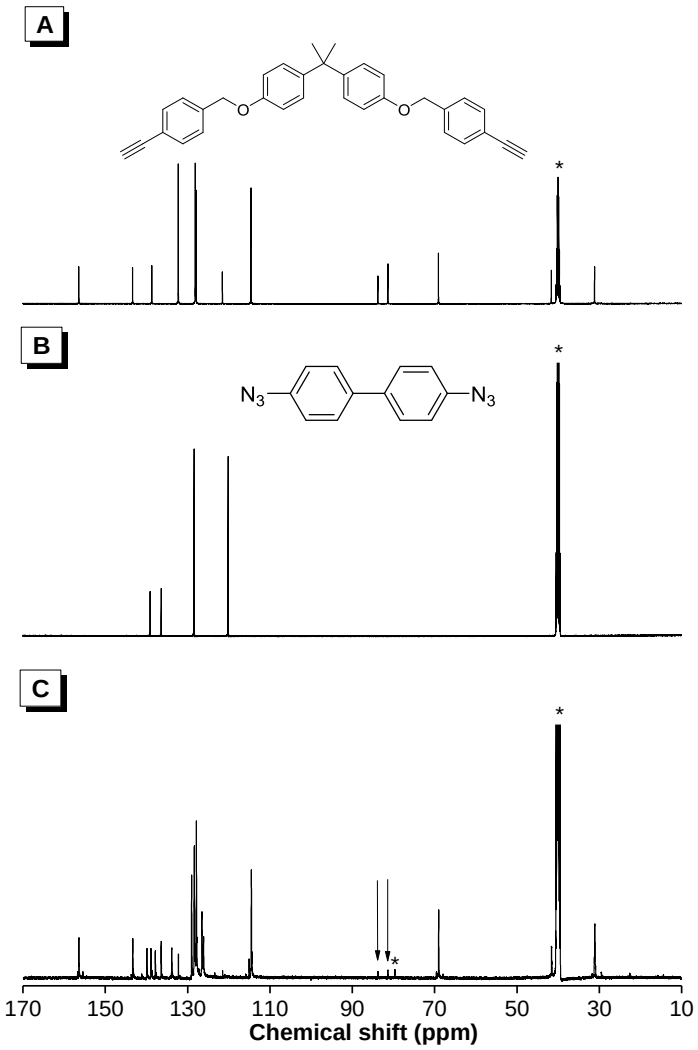

Figure S12. ^{13}C NMR spectra of **2a** (A), **1a** (B) and P**I** (C) in DMSO-d_6. The solvent peaks are marked with asterisks.

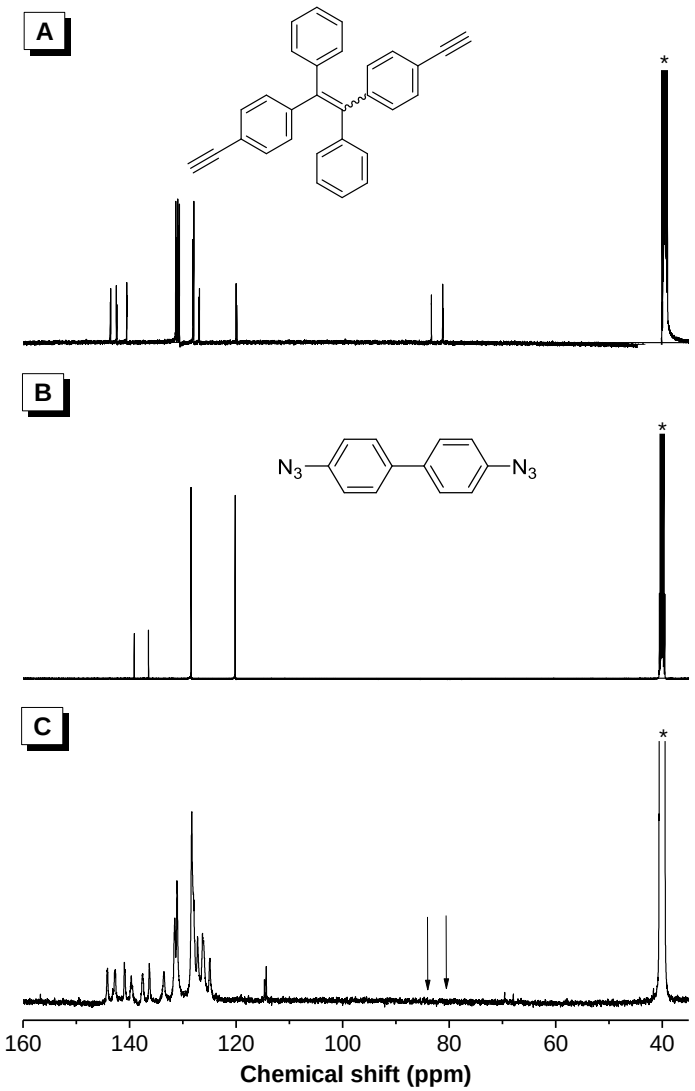

Figure S13. ^{13}C NMR spectra of **2b** (A), **1a** (B) and P**II** (C) in DMSO-d_6. The solvent peaks are marked with asterisks.

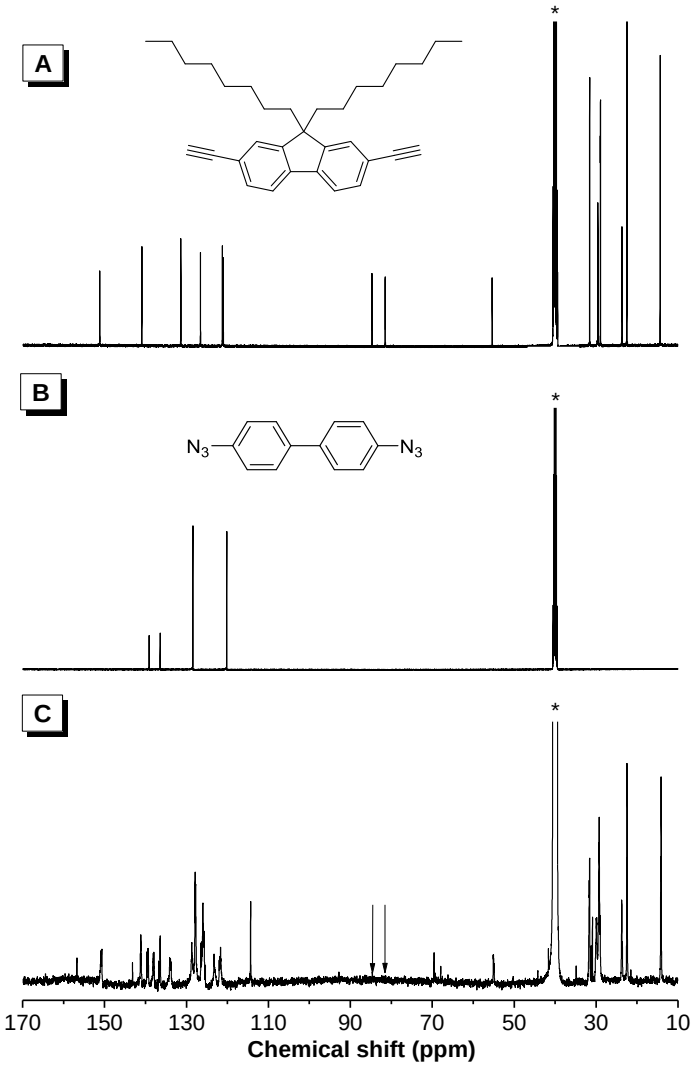

Figure S14. ^{13}C NMR spectra of **2c** (A), **1a** (B) and P**III** (C) in DMSO-d_6. The solvent peaks are marked with asterisks.

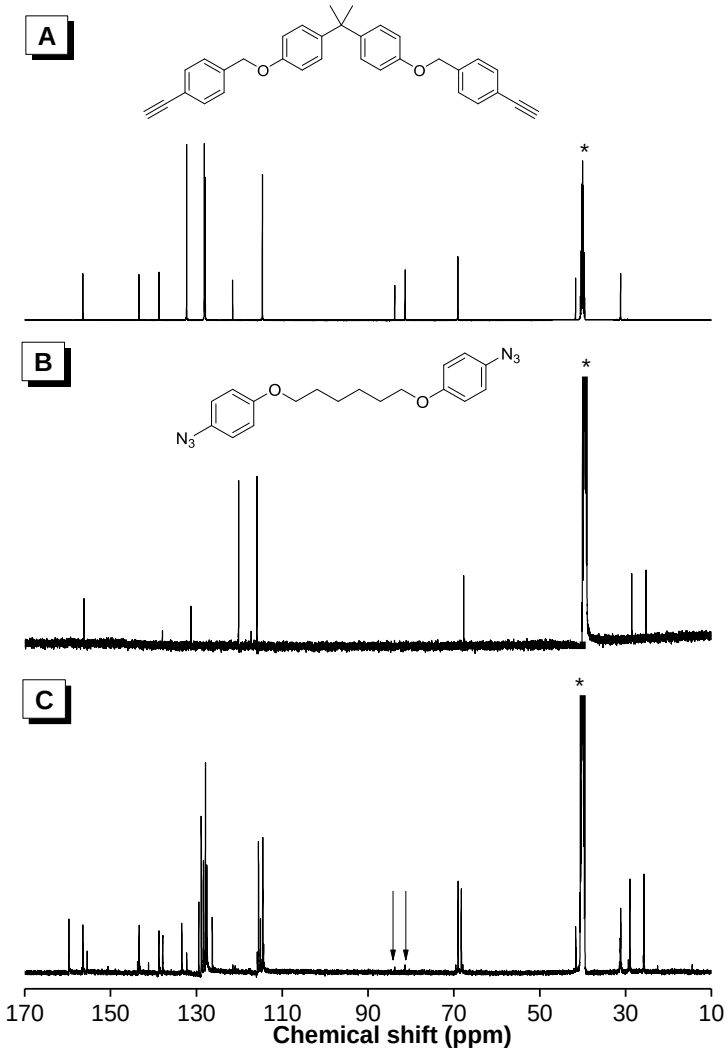

Figure S15. ^{13}C NMR spectra of **2a** (A), **1b** (B) and P**IV** (C) in DMSO-d_6. The solvent peaks are marked with asterisks.

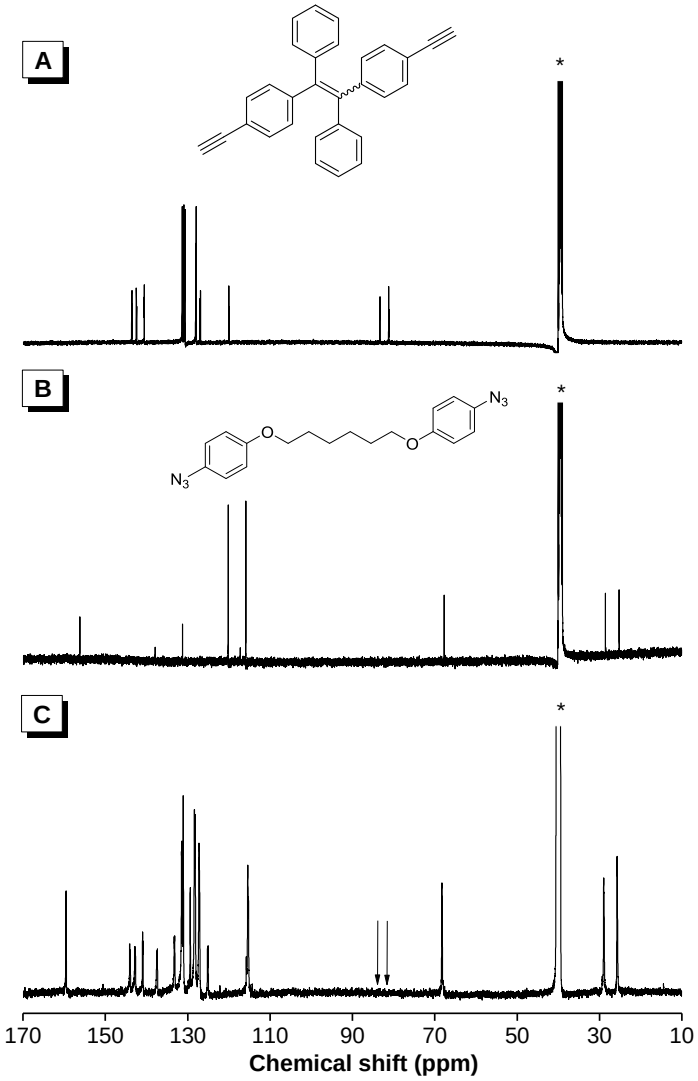

Figure S16. ^{13}C NMR spectra of **2b** (A), **1b** (B) and P**V** (C) in DMSO-d_6. The solvent peaks are marked with asterisks.

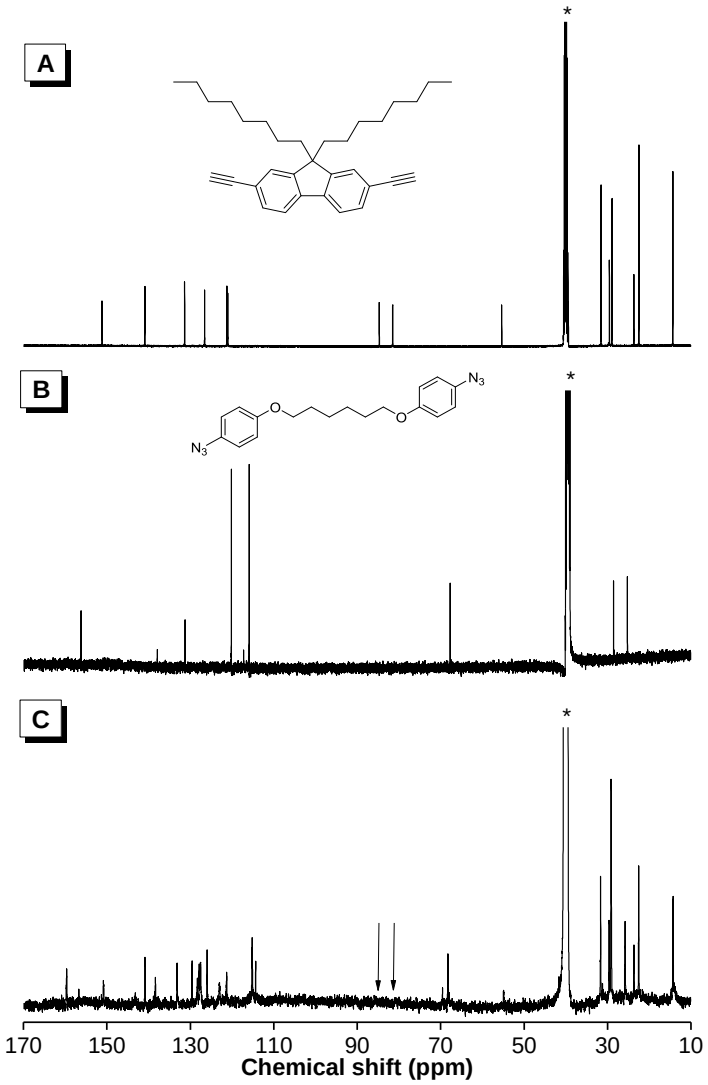

Figure S17. ^{13}C NMR spectra of **2c** (A), **1b** (B) and P**VI** (C) in DMSO-d_6. The solvent peaks are marked with asterisks.

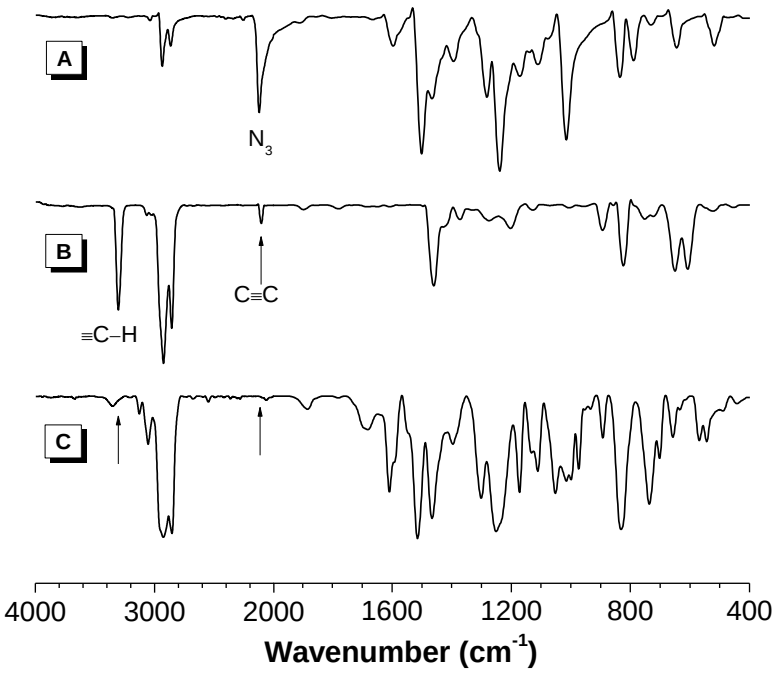

Figure S18. FT-IR spectra of **1b** (A), **2c** (B) and P**VI'** (C).

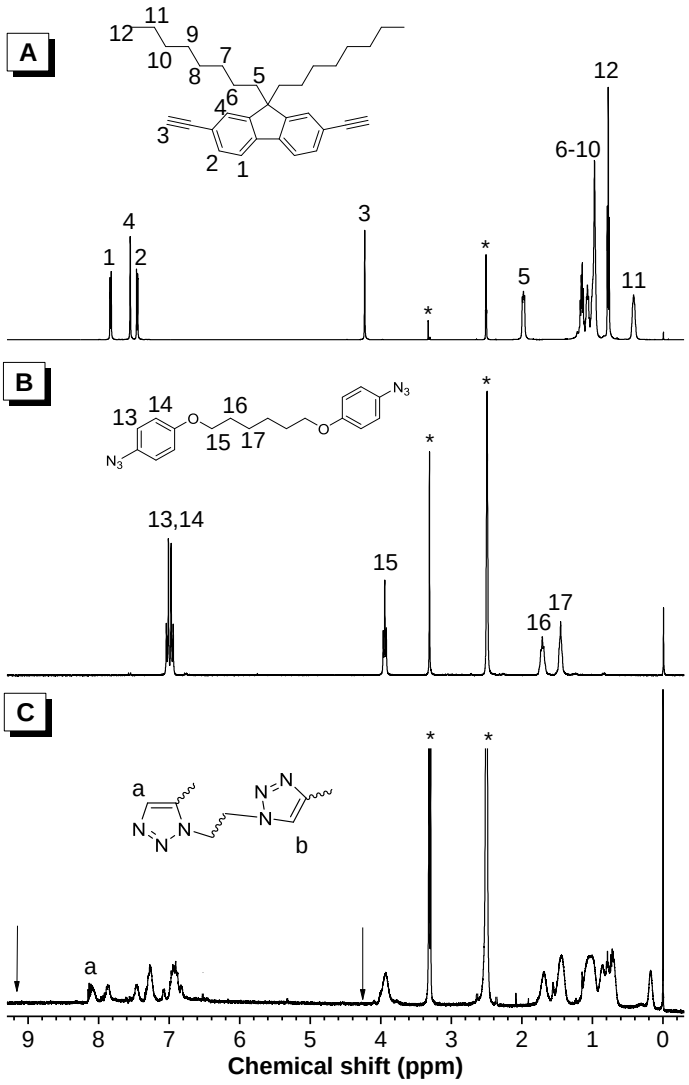

Figure S19. ^{1}H NMR spectra of **2c** (A), **1b** (B) and P**VI'** (C) in DMSO-d_6. The solvent peaks are marked with asterisks.

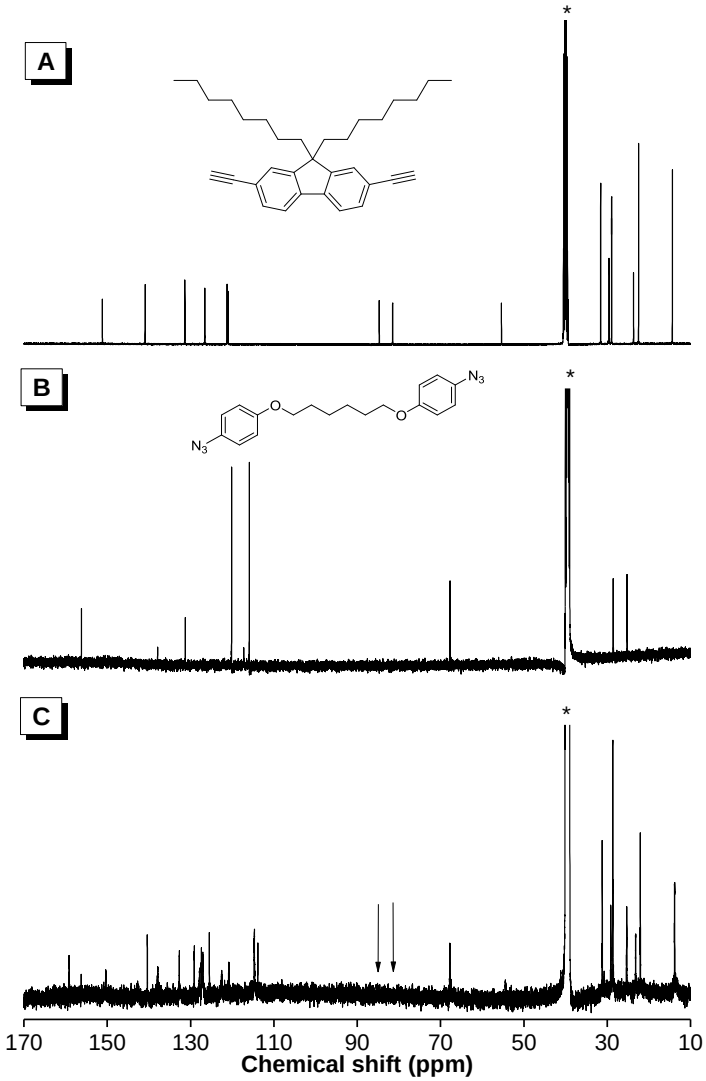

Figure S20. ^{13}C NMR spectra of **2c** (A), **1b** (B) and P**VI'** (C) in DMSO-d_6. The solvent peaks are marked with asterisks.

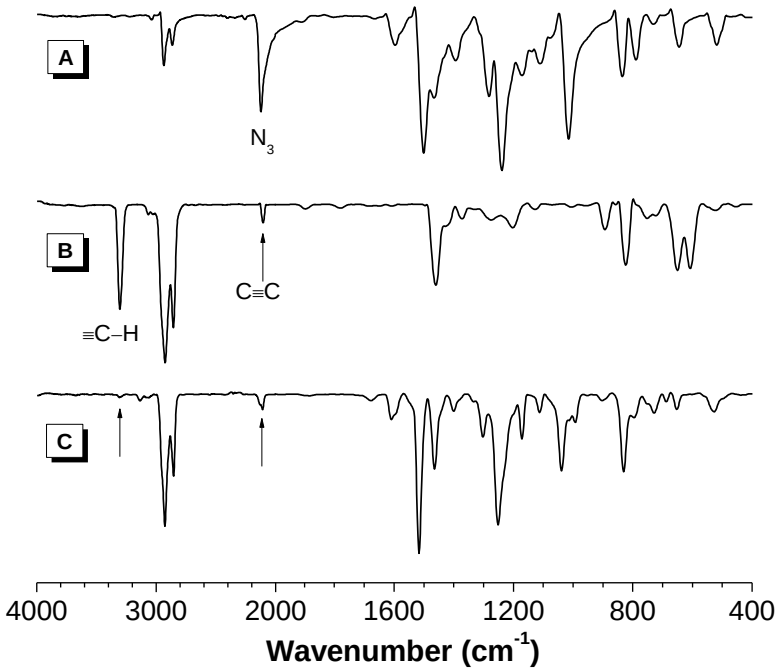

Figure S21. FT-IR spectra of **1b** (A), **2c** (B) and P**VII** (C).

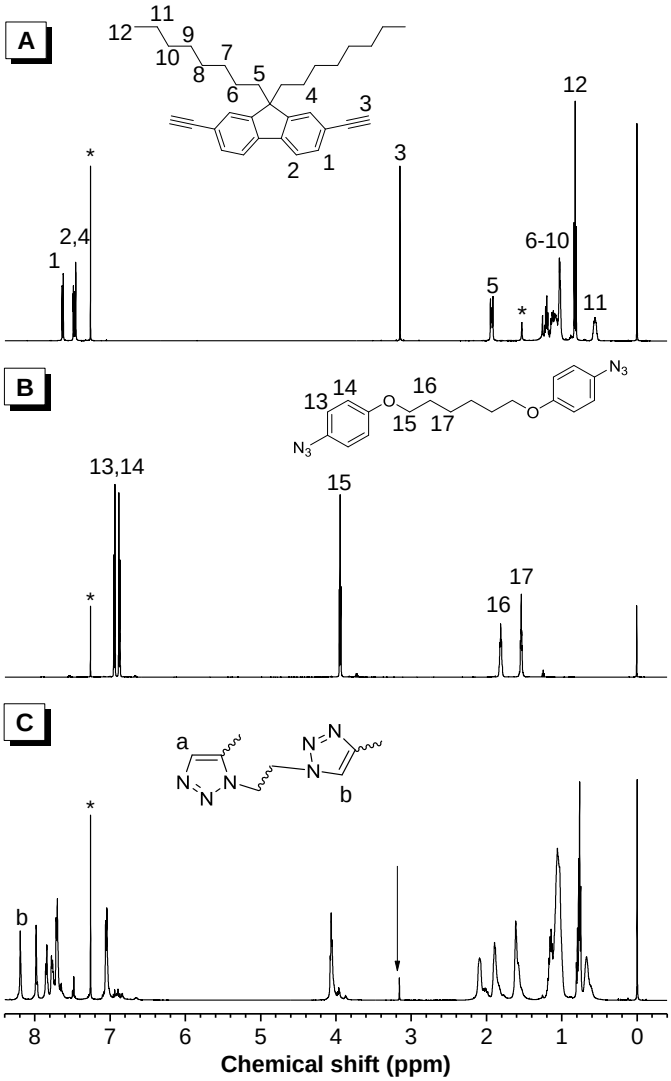

Figure S22. ^{1}H NMR spectra of **2c** (A), **1b** (B) and P**VII** (C) in $CDCl_3$. The solvent peaks are marked with asterisks.

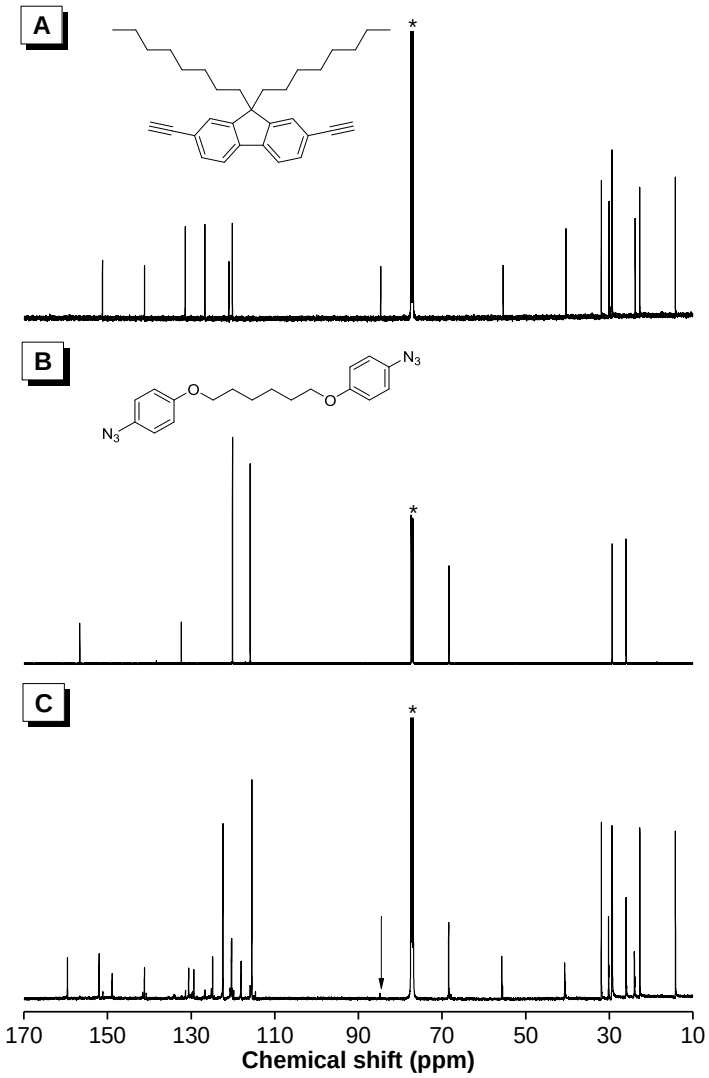

Figure S23. ^{13}C NMR spectra of **2c** (A), **1b** (B) and P**VII** (C) in $CDCl_3$. The solvent peaks are marked with asterisks.

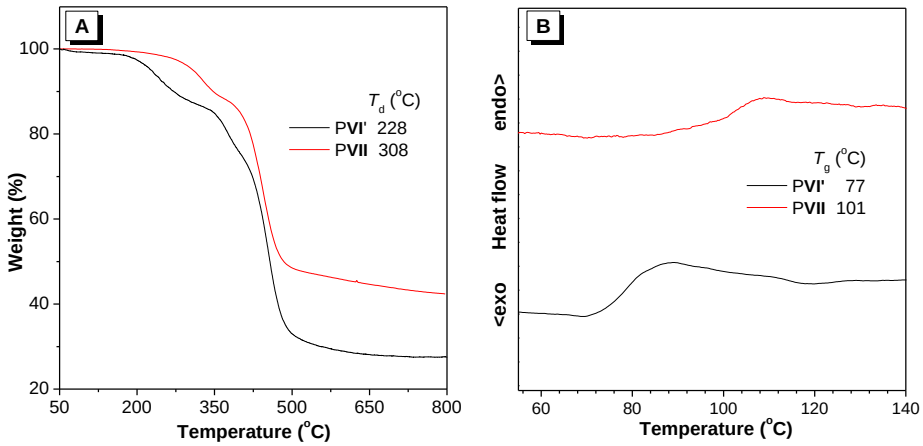

Figure S24. TGA (A) and DSC (B) curves of P**VI'** and P**VII** at a heating rate of (A) 20 °C/min and (B) 10 °C/min under nitrogen.

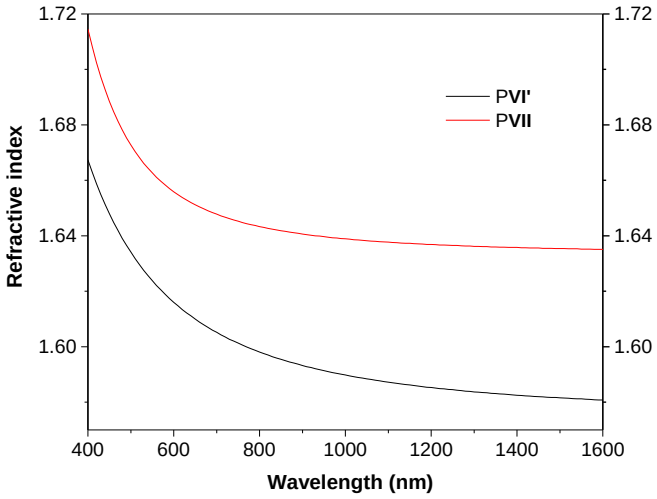

Figure S25. Light refraction spectra of thin solid films of P**VI'** and P**VII**.

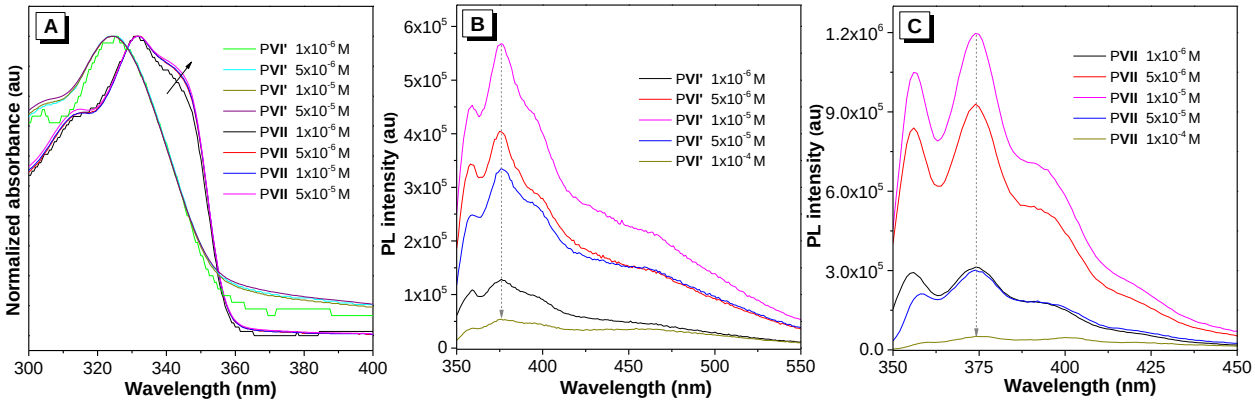

Figure S26. UV-vis absorption spectra of P**VI'** and P**VII** in THF solutions (A), PL spectra P**VI'** (B) and P**VII** (C) in THF solutions.

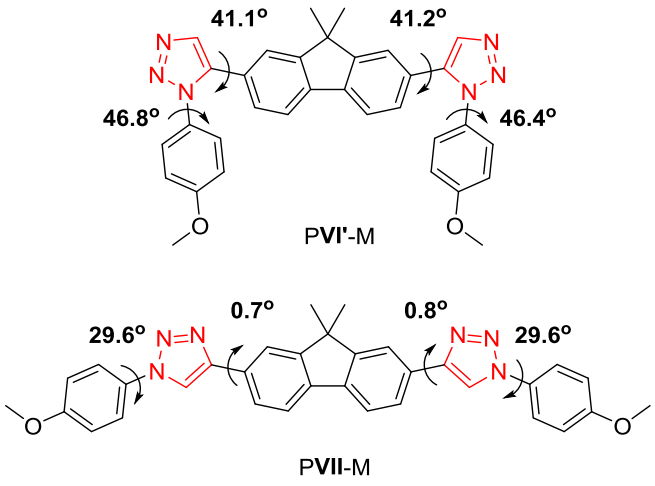

Figure S27. Dihedral angles of P**VI'**-M and P**VII**-M.

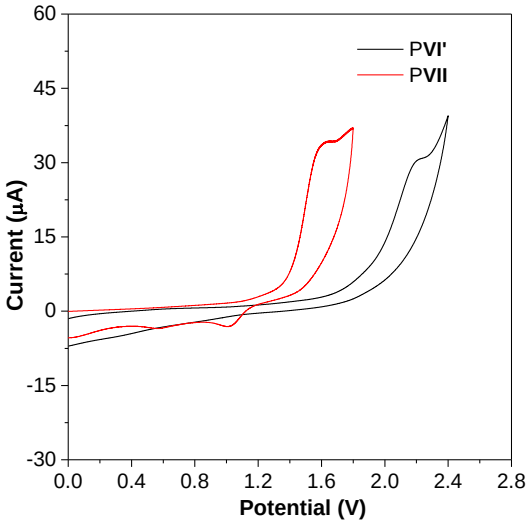

Figure S28. Cyclic voltammograms of **PVI'** and **PVII** with an $Hg/HgCl_2$ electrode as the reference electrode and an energy level of ferrocene of –4.40 eV as the internal standard.

Table S1. Photophysical and Calculated Results as well as Thermal Property of PVI' and PVII

entry	M_w[a]	$Đ$[a]	λ_{abs}[b] (nm)	Φ_F[c] (%)	τ (ns)	E_g[d] (eV)	T_g/T_d (°C)
PVI'	13 800	1.95	324	12.6	1.48	3.52	77/228
PVII	10 500	1.29	332	41.6	1.30	3.47	101/308

[a]Estimated by APC using THF as an eluant on the basis of a PS calibration; M_w = weight-average molecular weight; polydispersity index ($Đ$) = M_w/M_n; M_n = number-average molecular weight. [b]In THF solutions (10^{-5} M). [c]Absolute fluorescence quantum yield in THF solutions (10^{-5} M). [d]Estimated by optical band gap calculated from the onset of absorption spectra.

References

(1) Yuan, W.; Mahtab, F.; Gong, Y.; Yu, Z.; Lu, P.; Tang, Y.; Lam, J. W. Y.; Zhu, C.; Tang, B. Z. Synthesis and Self-Assembly of Tetraphenylethene and Biphenyl Based AIE-Active Triazoles. *J. Mater. Chem.* **2012**, *22*, 10472−10479.

(2) Liu, Y.; Wang, J.; Huang, D.; Zhang, J.; Guo, S.; Hu, R.; Zhao, Z.; Qin, A.; Tang, B. Z. Synthesis of 1,5-Regioregular Polytriazoles by Efficient NMe_4OH-Mediated Azide-Alkyne Click Polymerization. *Polym. Chem.* **2015**, *6*, 5545−5549.

(3) Wang, J.; Mei, J.; Yuan, W.; Lu, P.; Qin, A.; Sun, J. Z.; Ma, Y.; Tang, B. Z. Hyperbranched Polytriazoles with High Molecular Compressibility: Aggregation-Induced Emission and Superamplified Explosive Detection. *J. Mater. Chem.* **2011**, *21*, 4056−4059.

(4) Yao, B.; Mei, J.; Li, J.; Wang, J.; Wu, H.; Sun, J. Z.; Qin, A.; Tang, B. Z. Catalyst-Free Thiol-Yne Click Polymerization: A Powerful and Facile Tool for Preparation of Functional Poly(vinylene sulfide)s. *Macromolecule* **2014**, *47*, 1325−1333.

(5) Zhao, E.; Li, H.; Ling, J.; Wu, H.; Wang, J.; Zhang, S.; Lam, J. W. Y.; Sun, J. Z.; Qin, A.; Tang, B. Z. Structure-Dependent Emission of Polytriazoles. *Polym. Chem.* **2014**, *5*, 2301−2308.